Plasticity of visual looming response reveals a dissociation of innate and learned components

Authors

Paul B. Conway[1,2], Livia Autore[1,2,3], Andrea Muñoz Zamora[1,2], Antoine Harel[1,2], Arman A. Tavallaei[1,2], Stephen M. Winston[4,5], Clara Ortega-de San Luis[1,2,7], James D. O'Leary[1,2,8], Mark A. Brimble[6], Gisella Vetere[3], Tomás J. Ryan[1,2,8,9].

Affiliations

1 School of Biochemistry and Immunology, Trinity College Dublin, Dublin, Ireland
2 Trinity College Institute for Neuroscience, Trinity College Dublin, Dublin, Ireland
3 Cerebral Codes and Circuits Connectivity team, Brain Plasticity Unit, CNRS, ESPCI Paris, PSL Research University, France
4 Department of Surgery, St Jude Children's Research Hospital; Memphis, TN, 38105, USA.
5 Graduate School of Biomedical Sciences, St. Jude Children's Research Hospital; Memphis, TN, 38105, USA
6 Department of Host-Microbe Interactions, St. Jude Children's Research Hospital, Memphis, TN 38105, USA
7 Department of Health Sciences, University of Jaén, Jaén, Spain
8 Department of Neuroscience, Georgetown University Medical Center, Washington, DC, 20057, USA
7 Florey Institute of Neuroscience and Mental Health, Melbourne Brain Centre, University of Melbourne, Melbourne, Victoria, Australia
9 Child & Brain Development Program, Canadian Institute for Advanced Research (CIFAR), Toronto, Ontario, Canada

Correspondence: tomas.ryan@tcd.ie

Summary

Animals rely on both innate and learned behaviour to respond optimally to their environment. However, little is known about how the brain may reconcile the ability to produce hardwired responses essential to survival while still allowing for adaptive flexibility. Here, we demonstrate that innate looming stimulus responses, an innate predator-evasion behaviour, can be robustly extinguished via repeated unreinforced presentation over several days. We report that this extinction is long-lasting and generalises to other contexts, but can be rapidly recovered via the pairing of the visual stimulus with an aversive electric foot-shock stimulus. Moreover, fiber photometric recordings reveal that this behavioural paradigm results in the attenuation of SC and PAG physiological responses to visual looming stimuli, and that these responses do not recover following recovery of behavioural responses. An analysis of c-Fos expression patterns throughout the midbrain and hippocampus uncovered a ventral CA1 (vCA1) ensemble that is active during both innate and learned visual looming fear responses. We investigate the functional significance of this vCA1 ensemble and report that, while its activity is not necessary for innate defensive behaviour, it is necessary for learned fear responses. Together, these findings reveal a novel role of the hippocampus in enabling adaptive behavioural responses to the innately threatening visual looming stimulus which acts in complement with innate circuitry of the SC and PAG.

Introduction

Innate behaviours enable an animal to respond to ethologically salient stimuli without prior experience. This is particularly advantageous for threatening stimuli, as it allows the animal to engage in appropriate behaviour upon first encounter with the stimulus. However, over time the meaning of a given environmental cue can change, requiring the animal to adapt their responses through learning. This process causes changes in neuronal connectivity via plasticity mechanisms, and the enduring changes which encode this novel information are known as the memory engram (Josselyn and Tonegawa, 2020, Semon, 1921, Tonegawa et al., 2015). This raises an important question: how does the brain generate innate behavioural responses while still allowing for behavioural flexibility and learning?

A visual looming stimulus, such as an overhead expanding black disk which mimics an approaching aerial threat, can be used to trigger innate defensive responses of rodents such as freezing or fleeing towards shelter (Evans et al., 2018, Vale et al., 2020, Yilmaz and Meister, 2013). This innate behavioural response is crucial to the survival of the animal, and as such is highly conserved across species (Yilmaz and Meister, 2013, Carlile et al., 2006, Ingle and Karin, 1990, Wang et al., 1993, Schiff et al., 1962, Ball and Tronick, 1971, de Vries and Clandinin, 2012). Interestingly, the innate behavioural response to a looming stimulus has also shown experience-dependent plasticity. For example, mice can avoid areas where looming stimuli were previously presented, demonstrating associative learning (Evans et al., 2018, Burnett et al., 2024). Furthermore, the behavioural response can be prevented by initial presentation of a very low contrast stimulus and gradually increasing contrast, showing latent inhibition of this innate response (Lenzi et al., 2022, Mederos et al., 2024). Taken together, these studies suggest a role of learning in mediating adaptive defensive behaviours.

Recent work has shown that midbrain structures, particularly the superior colliculus (SC) and periaqueductal gray (PAG) (Lee et al., 2020, Evans et al., 2018, Shang et al., 2018, Deng et al., 2016, Fadok et al., 2017, Tovote et al., 2016, Kim et al., 2013) drive innate responses to looming stimuli, such as freezing and fleeing, by gating threat detection and response thresholds. The hippocampus is known to be involved in adaptive behavioural responses to learned threats (Liu et al., 2012, Zaki et al., 2022, Jimenez et al., 2020, Ortega-de San Luis et al., 2023, Kjelstrup et al., 2002), but it is not currently known if it may contribute to adaptive behavioural responses to innately threatening stimuli.

Here, we have designed a behavioural paradigm wherein visual looming threat responses are attenuated via repeated unreinforced presentation and rescued by pairing the stimulus with an electric foot shock. We report a loss in the responsiveness of the SC and PAG during visual looming stimulus presentation, which does not recover despite recovery of behavioural responses to the stimulus. Finally, we identify specific ensembles of cells in the ventral CA1 (vCA1) that are responsive to visual looming during naïve presentation, and later become necessary for rescued behavioural responses to the visual stimulus.

Results

Visual looming threat responses can be extinguished and recovered via learning

Visual looming presentation to mice evokes a rapid defensive behavioural response, characterised by fleeing to a shelter and unconditioned freezing (Fig. 1a). To investigate whether this innate behaviour can be modulated by learning, we established a behavioural paradigm where threat responses to visual looming stimuli could be modified by extinction training (figure 1a,b). In Pavlovian fear conditioning, repeated presentation of a conditioned stimulus (CS) in the absence of any reinforcing stimulus leads to the attenuation of the learned fear behaviour (Pavlov, 1927, Bouton, 2004). It can be hypothesised that the visual looming response consists of an innate association between the visual stimulus and an unconditioned response (Ryan et al., 2021).

To emulate fear extinction for an innate looming stimulus, mice were repeatedly presented with a looming stimulus over six days of training. In this assay the experimental group was exposed to 6 rounds of 15 visual looming stimuli, repeated over 6 days. A control group was placed into the arena for the same length of time each day but without presentation of the visual looming stimulus. On test 1 (pre-extinction) mice demonstrated a significant increase in both freezing and sheltering during looming stimulus presentation relative to pre-stimulus presentation (figure 1c-f). On test 2 (post-extinction), there was no significant increase in freezing or sheltering following stimulus presentation. In contrast, control mice maintained freezing and sheltering responses to the visual looming stimulus. These results demonstrate that innate fear responses to the visual looming response are plastic and can be attenuated via repeated presentation of the stimulus without any concurrent reinforcing stimulus.

In fear conditioning, extinction memories tend to be context-specific and spontaneously recover after a period of 3 weeks (Bouton and King, 1983, Rescorla, 2004). To test the former for visual looming extinction, mice were placed in a novel context following training and tested as before (supplementary figure 1d). In this case, mice retained similarly low levels of freezing and sheltering in both the familiar context and the novel context (supplementary figure 1e). To determine whether fear responses spontaneously recover, mice were tested 3 weeks after the end of the extinction training protocol (supplementary figure 1f). Mice maintained significantly lower levels of freezing and sheltering on test 3 relative to test 1 (supplementary figure 1g). These results show that the extinction-like phenotype of the visual looming response is resistant to recovery in conditions which typically elicit recovery of extinguished fear conditioned responses. This may reflect a high persistence of these adaptations, distinguishing it from extinction of classical fear conditioning.

To determine whether it is possible to recover looming threat response post-extinction training, a reinstatement training paradigm was designed. Following completion of the extinction training paradigm, mice received an additional training day where they were exposed to the looming stimulus paired with a co-terminating 2s electric foot shock (figure 1g). When mice were tested 24h later they showed a significant increase in freezing but not sheltering (figure 1h,i). Meanwhile, mice which were presented with either the looming stimulus or shock stimulus alone showed no significant increase in either freezing or sheltering (supplementary

figure 1h-m). As such, these results show that specific fear to the visual looming stimulus can be reinstated by pairing the visual stimulus with an electric foot shock.

SC and PAG responses attenuate with extinction and do not recover with reinstatement

Defensive behavioural responses to visual looming stimuli are known to be mediated by the accumulation of threat information in the deeper layers of the SC, which triggers the dorsal PAG to initiate a behavioural response (Evans et al., 2018). To understand how activity in these regions changes over the course of extinction and reinstatement, *in vivo* fiber photometry recordings were performed. The calcium indicator GCaMP6f was expressed via local injection of AAV9-Syn-GCaMP6f-WPRE-SV40, and calcium-dependent fluorescence was recorded via an optical fiber implant at the injection site through which 465 nm and 405 nm excitation light were simultaneously delivered. Recordings were performed in either the deep SC or the dorsal PAG (figure 2a,b). During innate looming responses in Test 1, visual looming stimuli reliably drive increases in activity of the deep SC. However in Test 2, following extinction, responses of the SC are diminished and these responses do not recover during Test 3 following reinstatement (figure 2c,d). A fast Fourier transform of the signal shows a strong peak at 1 Hz, coinciding with the frequency of looming stimulus presentation on Test 1, but not on Test 2 or 3 (figure 2e). As such, extinction training results in an attenuation of both looming threat responses and activity of the SC. Meanwhile, reinstatement training does not recover SC responses to visual looming stimuli, despite recovery of the behavioural responses.

These trends are mirrored in the PAG. The PAG shows a strong response to visual looming stimuli on Test 1, which attenuates by test 2, and remains suppressed on test 3 (figure 2h-i). Again, a fast Fourier transform of the signal on test 1 has a strong peak at 1Hz for Test 1, indicating that the activity is in synchrony with looming stimulus presentation, but not on Test 2 or 3 (figure 2j). As such, responses of the dorsal PAG are also diminished over the course of extinction training, and do not recover with reinstatement despite recovery of the behavioural responses. The separation of SC and PAG activity and looming behavioural responses, particularly freezing, are reflected by changes in correlation between these measures. On Test 1, a logistic regression of SC activity with freezing reveals a linear, negative correlation. This negative linear correlation persists until Test 2, but on Test 3 an inverse sigmoidal relationship develops, indicating that SC activity is suppressed during freezing (figure 2f). Meanwhile, the SC maintains a positive linear correlation with speed across all test days (figure 2g). This finding contrasts with mice that underwent “shock only” treatment during reinstatement training. Their activity on Test 3 shows no correlation with freezing behaviour (supplementary figure 2e), suggesting that the inverse relationship between freezing and SC activity is unique to the mice which have the shock stimulus paired with looming stimuli.

Dorsal PAG activity on test 1 is positively correlated with freezing during stimulus presentation, but not on test 2 and test 3 (figure 2k). As in the SC, the PAG develops an inverse sigmoidal relationship with freezing on Test 3. Meanwhile, PAG activity is positively correlated with speed, albeit not to the same degree as in the SC (figure 2l). These findings indicate that SC and PAG activity is attenuated with extinction learning. This activity is not recovered following reinstatement, highlighting a lasting effect of extinction learning in these regions and

suggesting that other brain regions may be responsible for the recovered behavioural response.

In summary, this data reveals a separation of threat responses to visual looming stimuli from SC and PAG activity as a result of extinction-reinstatement training. Therefore, another brain region must be implicated in the recovered threat responses of mice to the visual looming stimulus.

c-Fos expression patterns reveal persistent activity of a vCA1 ensemble following extinction-reinstatement

To investigate the activity of a wider range of brain areas in response to looming stimuli, c-Fos expression was analysed throughout the brain. TRAP2xAi32 mice (Allen et al., 2017, DeNardo et al., 2019) were used to tag neurons in a c-Fos dependent manner throughout the whole brain (figure 3a). TRAP2xAi32 mice underwent one of three training paradigms; re-exposure versus no re-exposure, to determine how naïve looming alters c-Fos expression; re-exposure following extinction training versus a control training, to determine the impact of extinction training; or re-exposure following extinction-reinstatement versus a control training to determine how reinstatement further changes c-Fos expression (figure 3b). Tagging was performed by delivering 4-OHT during naïve loom presentation, capturing the activity during innate loom responses. Following completion of the respective paradigm, mice were perfused 60min after looming stimulus presentation. Neurons positive for EYFP are those active during innate loom responses, neurons positive for endogenous c-Fos are those active during loom responses at the completion of the paradigm, and neurons which are positive for both EYFP and endogenous c-Fos are responsive during both loom presentations (figure 3b,c).

Following re-exposure to looming stimuli, no significant difference in overall c-Fos expression throughout the SC, PAG or hippocampus was observed when compared with no re-exposure mice (figure 3d). There was however a significant increase in the reactivation of previously labelled innately responsive cells in both the SCs and the vCA1 (figure 3e). This indicates that sparse ensembles in both regions contribute to the innate coding of the visual looming response. Following extinction training, there was a significant decrease in overall c-Fos expression in the deep SC (SCd), dorsolateral PAG (PAGdl) and lateral PAG (PAGl) compared with non-extinction controls (figure 3f). Meanwhile, the reactivation of innately responsive loom cells remains consistent throughout the SC, with a significant decrease in the PAGdm (figure 3g). As such, while there is a decrease in the overall activity of several midbrain regions, the activity of specific loom-responsive ensembles in the SC and hippocampus remains equal to innate controls. Following reinstatement training, overall c-Fos levels in the SC and PAG are consistent with innate controls, suggesting a recovery of c-Fos expression levels (figure 3h). This is in contrast with the lack of recovery of calcium-dependent fiber photometry signalling, perhaps indicating an increase of plasticity or partial recovery of these regions. There is a significant decrease in the reactivation of innately loom-responsive cells in the superficial SC (SCs), dorsomedial PAG (PAGdm), PAGdl and dorsal DG (dDG). Meanwhile, there is a significant increase in the reactivation of vCA1 cells which were active during innate loom responses (figure 3i). This suggests that reinstatement training specifically results in an attenuation of specific loom-responsive ensembles in the midbrain, but an upregulation of loom-responsive ensembles in the vCA1.

Together, these data demonstrate that the innate visual looming response increases activity of specific ensembles in the SC and ventral CA1. Moreover, following extinction there is reduced activity in the SC and PAG, while the ventral CA1 is equal to no-extinction controls. Following reinstatement, there is a recovery of overall c-Fos expression in the SC and PAG, but the activity of initially tagged innate loom-responsive cells does not recover. Meanwhile, there is increased reactivation of the initially tagged ventral CA1 loom-responsive cells. This suggests that the initially active vCA1 ensemble may also be implicated in the later reinstated threat responses to the visual looming stimuli in the absence of midbrain-driven responses.

Loom-responsive cells of the vCA1 are necessary for learned but not innate defensive behavioural responses

Based on the increased reactivation of innate-loom tagged vCA1 ensembles during both innate and reinstated loom threat response, alongside the established role of the vCA1 in fear conditioning reinstatement (Jimenez et al., 2020), the role of the vCA1 engrams in visual looming fear reinstatement was investigated. To determine whether specific loom-responsive cells in the vCA1 are necessary in the reinstated visual looming response, the f-FLiCRE labelling system (Kim et al., 2020, Pouget et al., 2024) was used. A viral cocktail containing AAV-Nrxn3b-Nav1.6-MKII-f-hLOV1-TEVcs(ENLYFQ/M)-tTA-VP16, AAV-GFP-CaM-uTEVp and AAV-TRE:mCherry-p2a-eNpHR was locally injected into the vCA1. Optical fiber implants were used to deliver light to the vCA1. This labelling paradigm relies on intracellular calcium alongside blue light (473 nm) to induce labelling of neurons using the tetracylcine transactivator (tTA), inducing expression of the destination construct (figure 4a-c). As a result, this system produces activity-dependent labelling during a dynamic window with a temporal precision on the order of seconds.

To investigate whether specific ensembles activate during reinstatement training are necessary for reinstated fear responses, vCA1 ensembles were tagged either pre-stimulus ("context label" or during loom and shock presentation ("loom label") of the reinstatement training session (figure 4d), inducing the expression of inhibitory Halorhodpsin. 24h later, mice were exposed to two rounds of looming stimulus presentation; first with laser stimulation at 595 nm to inhibit tagged cells and second with no light-induced inhibition. For cells tagged during "context labelling", there was a significant increase in freezing following loom-presentation regardless of whether the laser was on (test 3A) or off (test 3B) (figure 4e). However, for mice with cells tagged during loom and shock presentation, there was no increase in freezing whilst these cells were inhibited, but a significant increase in freezing when mice were presented the stimulus again without inhibition 90 s later (figure 4f). There was no significant difference in the number of cells tagged during these two sessions (supplementary 5a-c), despite their differing effect on behaviour. This indicates that there is a specific ensemble of cells in the ventral CA1 which is activated specifically during presentation of the looming and shock stimuli, which is necessary for recall of the reinstated fear 24h later.

Since looming and shock stimulus are presented together during reinstatement, this ventral CA1 ensemble may contain both loom-responsive and shock-responsive cells. However, histological analysis of c-Fos expression revealed an increase in loom-responsive cells tagged during naïve presentation (figure 3d-i). Because of this, we next investigated the functional significance of these loom-responsive ensembles of the vCA1 in the reinstated behavioural

response. Loom-responsive cells in the ventral CA1 were tagged using the f-FLiCRE system in naïve mice. Then, mice underwent the extinction-reinstatement training paradigm as before, except in this case each test day contained two rounds of looming stimulus presentation. During the first round, loom-responsive cells were optogenetically inhibited, and during the second round there was no inhibition applied (figure 4g). On Test 3, following reinstatement, there was no significant increase in freezing while loom-responsive cells were inhibited, but there was a significant increase in freezing to the looming stimulus 90s later when these cells were no longer being inhibited (figure 4h). As such, there are cells in the ventral CA1 which are active during innate visual looming responses but are not required for innate responses. However, these same cells are later necessary for recall of the reinstated visual looming fear responses.

Discussion

In this study, we establish a novel behavioural paradigm to explore how the brain facilitates adaptive responses to a highly innate, threat-related visual stimulus. We show that the innate visual looming response is subject to a long lasting and contextually generalisable extinction. However, threat responses to the visual stimulus can be recovered via pairing of the stimulus with an electric footshock. During extinction training, activity in the deep superior colliculus (SC) and dorsal periaqueductal gray (PAG) attenuate and do not recover after reinstatement. Furthermore, by analysing c-Fos expression in the midbrain and hippocampus, we have identified a population of vCA1 cells which respond to looming stimuli during naïve presentation, in addition to specific loom-responsive ensembles in the SC. Over the course of extinction-reinstatement, the specific loom-responsive cells of the SC no longer respond to the visual looming stimuli and this does not recover with reinstatement. Only the initially tagged vCA1 ensembles show a recovery of their response to looming stimuli following reinstatement training. Functional manipulation of these vCA1 ensembles revealed that these cells specifically respond to looming stimuli and are necessary for adaptive behavioural responses following reinstatement. This study revealed that the extinction and reinstatement of innate fear responses to a looming stimulus rely on hippocampus-dependent mechanisms. These findings demonstrate a novel adaptive pathway for the generation of innate behavioural responses while still allowing for behavioural flexibility and learning.

Adaptability of the innate looming response

Our visual looming extinction-reinstatement paradigm expands upon literature indicating that the innate looming response is adaptable. Prior studies show that spatial memory modulates flight behaviour via retrosplenial cortex-SC projections (Campagner et al., 2023). Mice can also remember areas where looming stimuli were previously presented to later avoid those areas (Evans et al., 2018), as well as learning to fear a tone previously paired with looming stimuli (albeit to a lesser degree than with an electric shock) (Heinemans and Moita, 2022). Additionally, gradual contrast increases in looming stimuli can reduce or abolish responses, highlighting stimulus-specific adaptation (Lenzi et al., 2022, Mederos et al., 2024). Our paradigm uniquely demonstrates a transition from looming-related fear to complete behavioural attenuation and, crucially, the reinstatement of fear responses to the same

looming stimulus, permitting within-subject comparisons of innate versus learned fear responses. The extinction phenotype characterised here has some distinctions from classical fear conditioning extinction. For example, it persists at least 3 weeks after extinction training and generalises to other contexts. As such, one may consider this a very persistent extinction memory. This phenomenon is also distinct from sensory habituation in several ways. Firstly, c-Fos analysis revealed continued responsiveness of specific loom-responsive ensembles in the superior colliculus post training, while habituation typically evoked a reduced activity in sensory processing regions (Thompson and Spencer, 1966, Rankin et al., 2009). Secondly, the ability of the mouse to learn an association between the visual looming stimulus and an electric foot shock demonstrates continued detection of the visual looming stimulus, even in the absence of a behavioural response. And thirdly, while a habituated response can typically be recovered by presentation of a startling stimulus on its own, an electric foot shock on its own is not sufficient to recover behavioural responses to the visual looming stimulus. Meanwhile, an electric foot-shock paired with the visual looming stimulus was sufficient to recover fear responses to visual looming stimuli. This learning occurred with only a single pairing of the looming stimulus with the shock, so is learned quite readily despite the otherwise persistent extinction memory.

A novel role for the hippocampus in adaptive looming responses

We identify a novel role for vCA1 in looming-evoked behaviour. Alongside canonical SC and PAG circuits, sparse vCA1 cells form looming-responsive engrams that are necessary for learned but not innate defensive behavioural responses to looming stimuli. These vCA1 loom-responsive engram cells are not necessary for evoking innate defensive behavioural responses, but do become necessary for learned responses following the extinction-reinstatement paradigm. Meanwhile, the SC and PAG responses which are known to drive visual looming fear responses at a population level (Evans et al., 2018) become much less responsive to visual looming stimuli and in fact have an inverse relationship with freezing. As such, it seems that the behavioural response to visual looming stimuli has transitioned from SC-dependency to vCA1-dependency.

The vCA1 is implicated in a wide range of emotionally-salient rapidly forming memories, including fear conditioning (Ortega-de San Luis et al., 2023, Jimenez et al., 2020, Shpokayte et al., 2022, Zaki et al., 2022), social memory (Okuyama et al., 2016) and reward (Ruediger et al., 2012, Shpokayte et al., 2022). Therefore, these loom-responsive stimuli in the vCA1 may aid in adaptation of behaviour in response to looming stimuli, such as avoiding areas where looming stimuli were previously presented (Evans et al., 2018, Burnett et al., 2024).

Insights into instinct and memory interactions

In summary, the SC and PAG mediate rapid, defensive looming responses, reflecting the evolutionary importance of these circuits. However, the brain balances this hard-wired response with adaptive flexibility, storing looming-related information in the hippocampus to accommodate new experiences. This strategy likely reflects selection pressures on rapid, innate threat responses where immediate action is critical and learning opportunities are minimal. By recruiting vCA1 for adaptive learning, the brain can accommodate plasticity of behaviour without compromising rigid survival circuits. Thus, the looming response exemplifies how even highly innate, survival-critical behaviours maintain plasticity, blending instinct with the flexibility afforded by memory systems.

Methods

Animals

All wild-type behaviour, fiber photometry and f-FLiCRE experiments were performed with C57BL/6J mice. Whole-brain engram labelling experiments were performed with TRAP2 x Ai32 (Allen et al., 2017, DeNardo et al., 2019, Madisen et al., 2010). Mice were housed in groups of 3-6 in cages with enrichment, food and water ad libitum under a 12 h light/dark cycle. The animal room was kept at a constant temperature of 22°C and 50% humidity. Mice used for experiments were approximately 8-12 weeks of age. All experiments were performed during the light phase. All experimental manipulations were carried out accordingly with Health Products Regulatory Authority (HPRA) Ireland guidelines and the principle of the 3R's (https://nc3rs.org.uk/) and with ethical approval from the Trinity College Dublin ethics committee andthe Animal Research Ethics Committee from the Health Products Regulatory Authority (HPRA).

Visual looming presentation

The looming behavioural arena consisted of a rectangular floor (46 cm width x 30 cm length) and a computer monitor on top (28cm above). A red polycarbonate tube (7.5 cm diameter x 15 cm length) was positioned at the centre of the rear wall to provide a shelter. One day prior to experiments, mice were habituated to the arena for 5 min while the monitor displayed a white image. On experimental day, after 5 min of acclimation with a white monitor, the looming stimulus was triggered when the animals were located in the half of the arena opposite the shelter. The stimulus consisted in black disc appearing in the centre of the monitor at a diameter of 2 degrees of visual angle, expanding to 20 degrees in 250 ms, remaining at that size for 250 ms before disappearing. This was repeated 15 times with 500 ms between repetitions. After 15 presentations, the mice were left in the arena with a white monitor for 1 min before being taken back to their home cage. The arena and the shelter were cleaned with Trigene between animals. Custom Python code using the PsychoPy library (Peirce, 2009) was used to present stimuli and record video of the animals. Time spent freezing and sheltering were scored using DeepLabCut tracking (Mathis et al., 2018). Sheltering was defined as having all body parts (excluding the tail) within the y-axis limits of the shelter, and at least half of all body parts (excluding the tail) contained within the x-axis limits of the shelter. Freezing was defined as periods in which no more than 1 body part was detected as moving a distance of 2mm or greater, for a time period of at least 0.5s. DeepLabCut behavioural scoring was verified by manual scoring in all wild type experiments.

Visual looming extinction

After habituation day and looming test 1 described above, mice were repeatedly exposed to three waves of 15 looming stimulus presentations, separated by 1 min each, or a white screen control for the same length of time on 6 consecutive days in the absence of the shelter. On the following days, mice underwent looming test 2, with the same parameters as test 1, the shelter being present.

Visual looming reinstatement

After completing the extinction paradigm, mice received an additional training day in the visual looming assay without a shelter. After a 5min habituation period, mice were either presented with a train of 15 looming stimuli paired with a co-terminating 0.75mA 2s foot-shock, or just the foot-shock without visual stimulus presentation. Mice were then test 24h later with a shelter**.**

Stereotactic surgery

Stereotactic surgery was performed at least two weeks before starting any behavioural procedures. Mice were anaesthetized with 500 mg kg^{-1} avertin and head fixed on the stereotaxic instrument. Ophthalmic ointment was applied to eyes in order to prevent drying and intracutaneous lidocaine was injected in the skull. The surgical area was then washed with chlorohexidine and 70% ethanol three times before using a blade to perform a 1-1.5 cm incision through the midline of the scalp. After swabbing with increasing concentrations of ethanol, hydrogen peroxide was used to enhance visualisation of lambda and bregma. Animals underwent bilateral craniotomy and holes were drilled at the appropriate coordinates for the target region, detailed below. The viral mix was injected using a micro syringe pump (UMP3;WPI) and a 10 µL Hamilton syringe (701LT; Hamilton) at the appropriate depth for the target region. Injection of virus was at a rate of 60 nL/min. After completion of the injection, the needle was left in the injection site for an additional 5 minutes. For optogenetic experiments, a fiber implant (Doric) was fixed to the stereotaxic adapter and was lowered in the brain, 0.1-0.2mm above virus injection site. To secure the implant, an even layer of Metabond was applied and let dry for about 10-15 minutes. Dental cement was then used to secure the cap to the implant. The protective cap was provided by cutting the top portion of a black polypropylene microcentrifuge tube. Animals were then left in a warm box (29°C) until recovered from anaesthesia and then were returned to their homecage. On the day of the surgery and on the two following days mice were injected subcutaneously with meloxicam (0.075 mL/5g). Mice were allowed to recover for 14 days before any behavioural procedure was performed. Recovery was monitored with the use of a HPRA-approved recovery assessment table.

Viruses

pAAV.Syn.GCaMP6f.WPRE.SV40 was a gift from Douglas Kim & GENIE Project (Addgene plasmid # 100837-AAV9 ; http://n2t.net/addgene:100837 ; RRID:Addgene_100837)
Plasmids for AAV-TRE:mCherry-p2a-eNpHR, AAV-GFP-CaM-uTEVp and AAV-Nrxn3b-Nav1.6-MKII-f-hLOV1-TEVcs(ENLYFQ/M)-tTA-VP16 were a gift from Alice Ting. Viral vectors were produced and purified by Mark Brimble and Stephen Winston as previously described (Pouget et al., 2024).

Virus	Addgene ref	Serotype	Titer	Dilution	Paper reference
AAV9-Syn-GCamp6f	#100837	AAV9	≥ 1×10^{13} vg/mL	1 in 2	(Chen et al., 2013)

AAV-TRE:mCherry-p2a-eNpHR (f-FliCRE 1)	#158703	AAV-DJ	≥ 1×10^{13} vg/mL	undiluted	(Kim et al., 2020)
AAV-GFP-CaM-uTEVp (f-FLiCRE 2)	#163032	AAV-DJ	≥ 1×10^{13} vg/mL	undiluted	(Kim et al., 2020)
AAV-Nrxn3b-Nav1.6-MKII-f-hLOV1-TEVcs(ENLYFQ/M)-tTA-VP16 (f-FLiCRE 3)	#163031	AAV-DJ	≥ 1×10^{13} vg/mL	undiluted	(Kim et al., 2020)

In vivo fiber photometry

A single-site, two-colour fiber photometry system (Doric Lenses) was used for *in vivo* fiber photometry, adapting the protocol of (Silva et al., 2021). Recordings were taken of the 405nm isosbestic calcium-independent signal and the 465nm calcium-dependent GCaMP6f fluorescence. The LED power was constant across animals and experimental sessions (200mW). The presence of visual looming stimuli was synchronised with fluorescence recordings via a transistor-transistor logic pulse from an Arduino module. Animals were habituated to patch chords in a familiar environment (not recorded) and in the looming environment (recorded) for 5min each over the two days prior to the commencement of the extinction-reinstatement training paradigm.
Acquired data files were processed using code adapted from (Martianova et al., 2019). A moving mean was applied to smooth the signal. And baseline correction was performed using the adaptive iteratively reweighted Penalised Least Squares (airPLS) algorithm to remove the slope and low frequency fluctuations in the signal. Each signal was normalised according to the mean and standard deviation. Using non-negative robust linear regression, the normalised 405 signal was fit to the 465 signal, in the format y=a*x+b. The parameters of this regression (a,b) were used to calculate new values for the 405 signal fitted to the 465 signal. Finally, the normalised fluorescence dF/F (z dF/F) is calculated as the normalised 465 signal subtracting the fitted normalised 405 signal.

TRAP2xAi32 engram labelling

TRAP2xAi32 were placed in the visual looming assay for a 5 minute acclimation period before presentation of any stimuli. Three rounds of 15 looming stimuli were presented at a frequency of 1 loom per second, with a 1 minute rest period between rounds. Immediately following the end of the exposure paradigm, mice were intraperitoneally injected with 4-hydroxtamoxifen (4-OHT; Sigma Aldrich) at a dosage of 50 mg/kg to transiently induce labelling in cells in a c-Fos-dependent manner.. All 4-OHT was freshly prepared on the labeling day in a mix of sunflower seed oil and castor oil (4:1, Sigma-Aldrich) at 10 mg/ml.

f-FLiCRE engram labelling and stimulation

Mice were injected with a 1:1:1 viral cocktail including AAV-TRE:mCherry-p2a-eNpHR, AAV-GFP-CaM-uTEVp, and AAV-Nrxn3b-Nav1.6-MKII-f-hLOV1-TEVcs(ENLYFQ/M)-tTA-VP16 in

the ventral CA1. This viral cocktail allows expression of the f-FLiCRE labelling paradigm, which will result in expression of the inhibitory halodrhodopsin eNpHR upon coincidence of blue light (473nm) and calcium. For tagging of cells during the reinstatement training session, mice initiated the extinction-reinstatement training paradigm 3 weeks post-surgery. On the reinstatement training session, the blur laser was turned on for a 75s period either beginning 1 minute into the acclimation session, or at the onset of visual stimulus presentation. Light stimulation was delivered via continuous wave at a power of 5mW. The following day, mice underwent 2 rounds of visual stimulus presentation separated by at least 90s. On the first round, a yellow laser (595 nm) was turned on to inhibit cells from 30s pre-stimulus until 30s post-stimulus onset. Laser stimulation was performed at 10Hz with 20ms pulses, at a power of 5mW. On the second round, no light was turned on.
For mice tagged during innate loom presentation, mice were presented with looming stimuli before any training commenced and tagged via the same protocol. Mice then commenced the extinction-reinstatement training paradigm, with two rounds of visual looming stimuli, receiving yellow light inhibition for the first round and no inhibition for the second.

Immunohistochemistry

Mice were injected intraperitoneally with a terminal dose of Sodium Pentobarbital (50 µL) and perfused transcardially with PBS followed by 4% paraformaldehyde. Brains were then collected and left in 4% PFA at room temperature for 24 h, after which they were moved to PBS and stored at 4°C. Brains were cut using a vibratome into 50 µm coronal slices for all experiments except for whole brain imaging experiments, which were cut into 100 µm coronal slices.
For the immunostaining, slices were first washed in PBT 0.2% three times for 10 minutes. Then, they were incubated in a blocking solution (PBT 0.2% + NGS 10%) for 1 hour at room temperature. They were incubated with primary antibody (in PBT 0.2% +NGS 3%) overnight at 4°C while shaking. On the following day, slices underwent three 10 min washes in PBT-0.2% before incubation with secondary antibody (PBT 0.2% + NGS 3%) for two hours in the dark at room temperature. Then, after three additional 10 min washes in PBT 0.2%, slices were stained with DAPI (1:1000 in PBS) for 15 minutes at room temperature. Slices were finally mounted on superfrost slides using Vectashield-DAPI. The antibodies used for the c-Fos staining were rabbit anti-c-Fos (Synaptic Systems #226008 at 1:1000) and anti-rabbit Alexa-568 (Invitrogen) (1:500). ChR2-EYFP was stained using a primary chicken anti-GFP IgY fraction (Invitrogen) (1:500) and rabbit anti-chicken Alexa-488 IgG (Invitrogen) (1:500).

Image Acquisition and Analysis

Images were taken on a laser confocal microscope (Leica SP8 gated STED) with a 20x magnification unless otherwise stated. At least 4 images were taken for each region of interest per mouse. When the implant was not targeted correctly into the region of interest the animal was excluded from subsequent analysis. For each region of interest, density of cells was estimated by sampling cell density in the region of interest to calculate the number of DAPI cells per μm^2. The total number of cells in a region was calculated by multiplying this value by the total area of the region counted. The number of c-Fos positive cells was manually counted using ImageJ.

Statistical Analysis

Statistical analysis was performed using the pingouin and scipy.stats packages on Python. Data was tested for normality using the Shapiro-Wilk test. An unpaired Student's T-test was used to compare means of two independent groups that assume equal variance between groups, while the paired test was used for dependent groups. For data with more than two groups, an ANOVA was performed to determine if there was a significant difference. If so, and the data was normally distributed, post-hoc analyses were performed for pairwise comparisons. For data with multiple comparisons from the same subjects, False discovery rate correction via the Benjamini-Hochberg method was performed to calculate adjusted q values.

Figure Titles and Legends

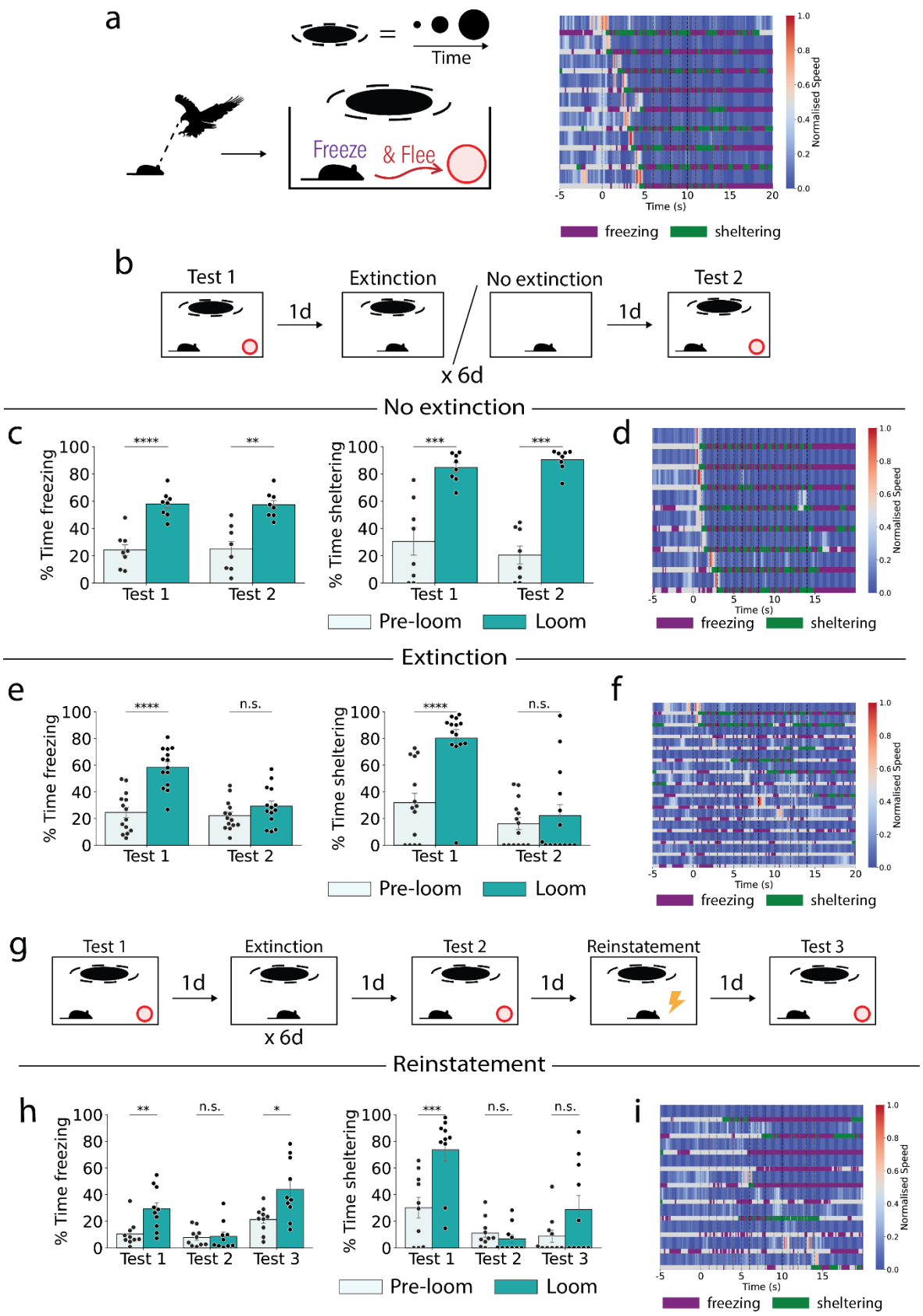

Figure 1 Extinction and reinstatement of innate visual looming fear responses. (a) Behavioural paradigm to test fear responses to visual looming stimuli. The heatmap indicates speed, with each blue-red row indicating the speed of a single mouse (n = 9 mice). Beneath the speed, a bar indicates whether the individual mouse was detected as freezing (purple) or sheltering (green). Looming stimulus onset is indicated by the dashed black lines, with first stimulus at time=0s. (b) Behavioural paradigm for extinction training. (c) Freezing and sheltering behaviour of the no-extinction cohort, 30s pre- and post-stimulus onset (Student's paired t test; n = 8 mice). (d) Heatmap indicating speed for the no extinction cohort, which each row indicting a single trial. Sheltering is indicated in green, and freezing is indicated in purple. (e-f) As in c-d, but for the extinction cohort (n = 14 mice). (g) Extinction-reinstatement training paradigm. (h) Freezing and sheltering responses of mice following reinstatement via pairing of the looming stimulus with a shock (Repeated measures ANOVA and posthoc Student's paired T test; n = 10 mice). (i) Heatmap indicating speed for the no extinction cohort, which each row indicting a single trial. n.s. $p \geq 0.05$, *$p<0.05$, **$p<0.01$, ***$p<0.001$, ****$p<0.0001$

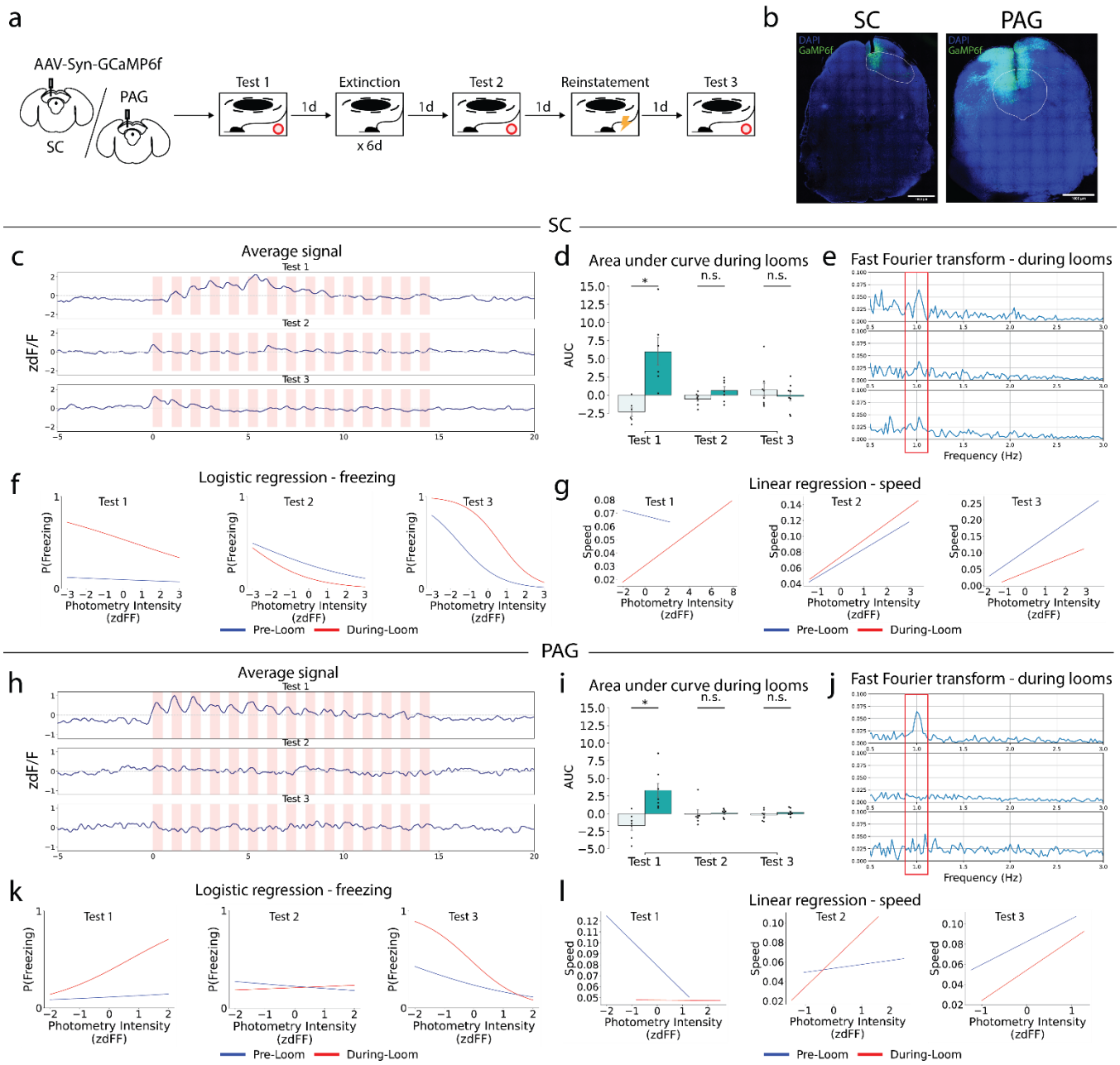

Figure 2 Extinction attenuates SC and PAG looming stimulus responses which do not recover with reinstatement training. (a) GCaMP was virally expressed in the SC or PAG. Fiber photometric recordings of GCaMP fluorescence were taken over the course of the extinction-reinstatement training paradigm. (b) Example histology from slices expressing GCaMP in the SC or PAG. (c) Mean traces of calcium activity in the deep SC on each test day (n = 6 mice). (d) Area under curve of GCaMP signal 15s pre- and post-stimulus onset, for each day (Student's T test). (e) Fast Fourier transform of the GCaMP signal during stimulus presentation on each day. The most ethologically relevant peak occurs is at 1Hz, which is the frequency of looming stimulus presentation. (f) Logistic regression of freezing probability with GCaMP signal, 15s pre- and post-stimulus onset, for each test day. (g) Linear regression of speed with GCaMP signal, 15s pre- and post-stimulus onset, for each day. (h-l) As in c-g, but with recordings taken from the PAG (n = 7 mice). n.s. p≥0.05, **p<0.001

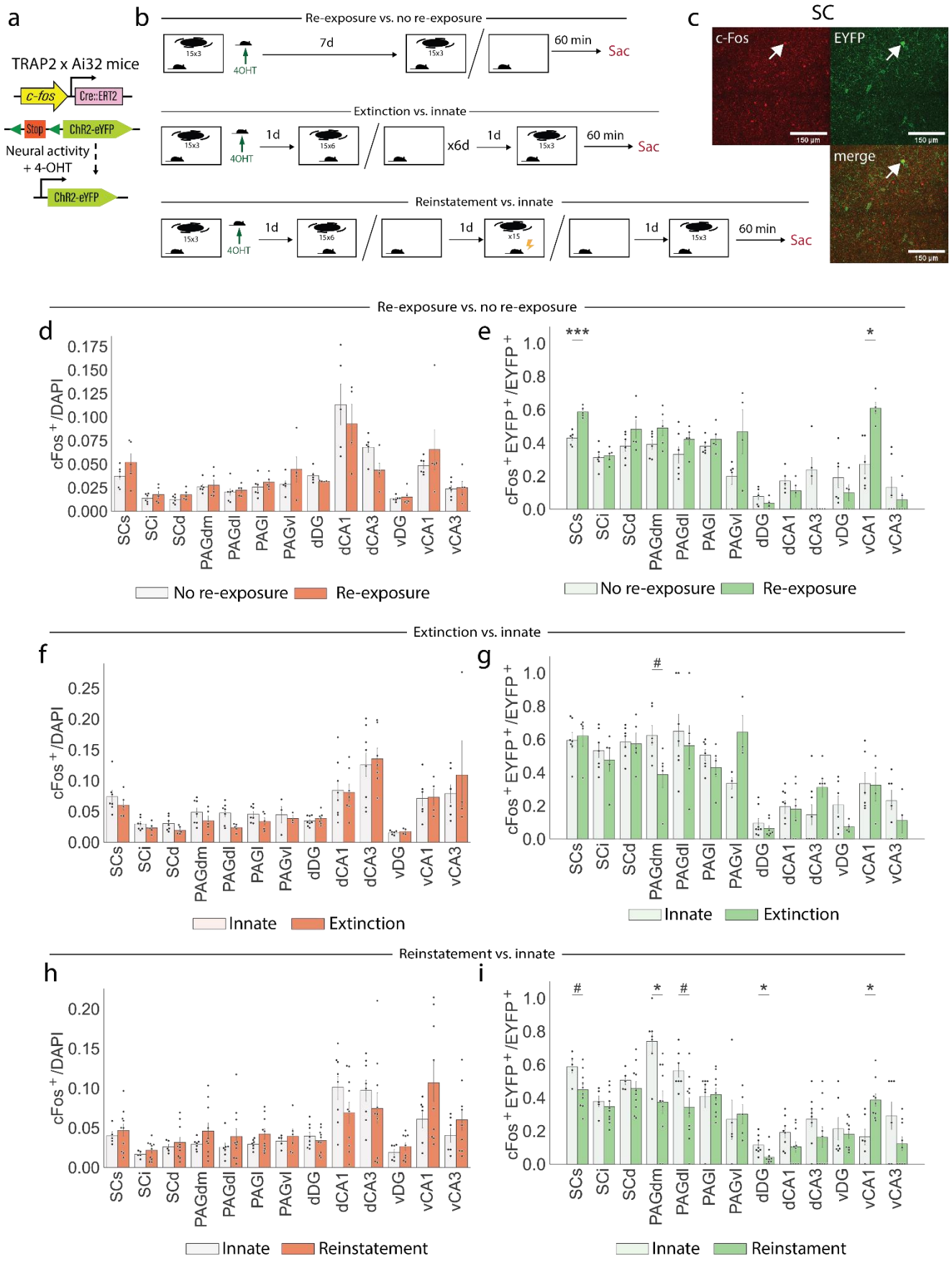

Figure 3 Patterns of c-Fos expression in the SC, PAG and HPC reveal a loss of activity in the SC and PAG following extinction-reinstatement but persistent activity of the

vCA1. (a) Engram labelling strategy. (b) TRAP2xAi32 mice underwent one of three types of behavioural paradigms; re-exposure (n = 6 mice) vs. no re-exposure (n = 6 mice), extinction (n = 7 mice) vs. innate (n = 8 mice), or reinstatement (n = 11 mice) vs. innate (n = 8 mice). Mice were injected with 4-OHT to transiently induce c-Fos dependent EYFP upon first exposure to the looming stimulus, and later perfused 60min following stimulus presentation at the end of the behavioural paradigm. (c) Example histology from the SC, with an $EYFP^{+}$c-Fos^{+} cell highlighted by the white arrow. (d) c-Fos expression upon completion of the re-exposure vs. no re-exposure paradigm (Student's unpaired t test with False discovery rate correction). (e) Proportion of initially tagged $EYFP^{+}$ cells which also express c-Fos upon completion of the re-exposure vs. no re-exposure paradigm (Student's unpaired t test with False discovery rate correction). (f-g) As in d-e, but for the extinction vs. innate paradigm. (h-i) As in d-e, but for the reinstatement vs. innate paradigm. n.s. $p \geq 0.05$, # $p<0.05$, * $q<0.05$, ** $q<0.01$, *** $q<0.001$; where p is the Student's t test p value, and q is the false discovery rate-adjusted p value.

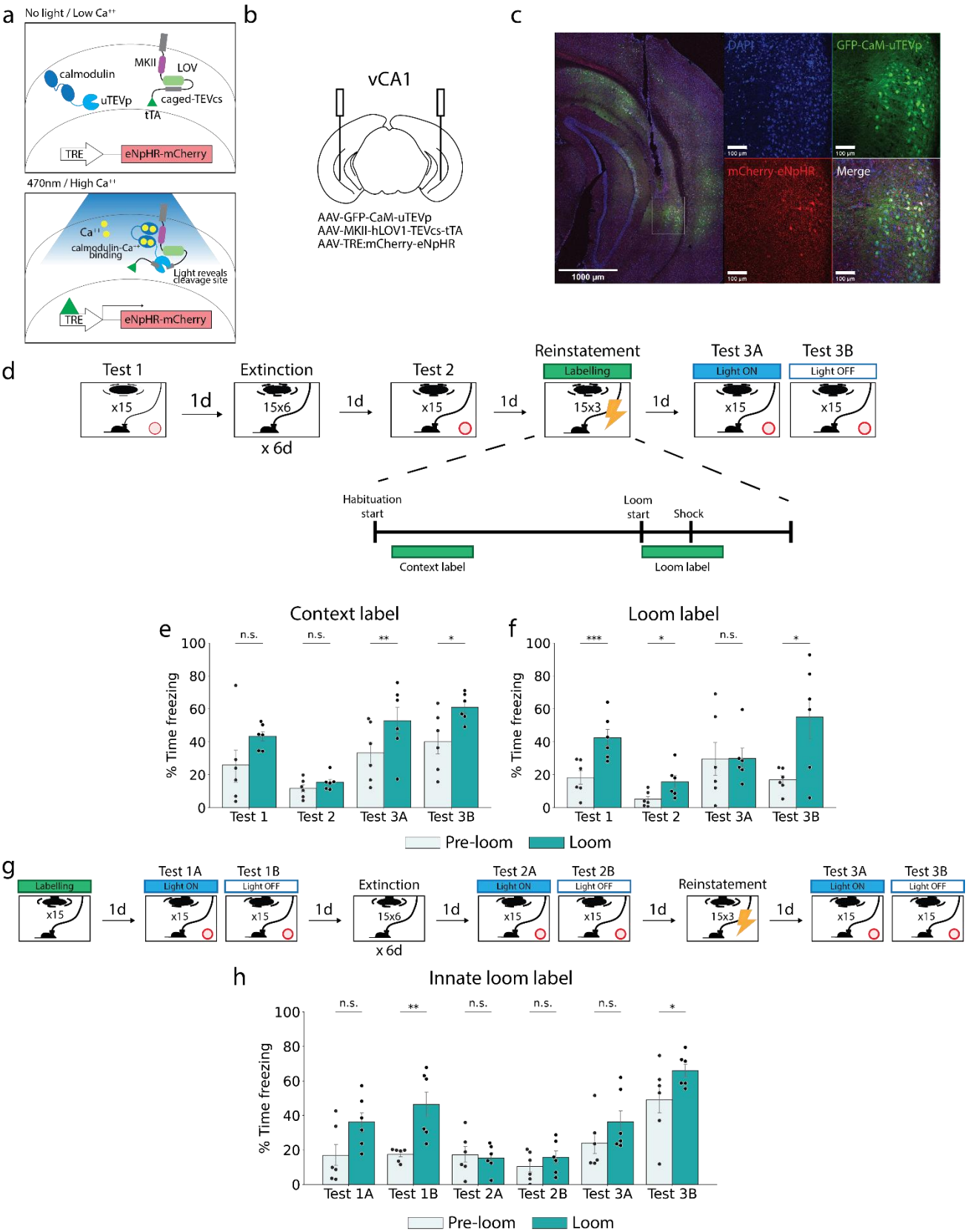

Figure 4 Loom-responsive cells in the ventral CA1 are necessary for reinstated but not innate visual looming fear responses. (a) f-FLiCRE labelling system. The coincident presence of calcium and blue light enables expression of eNPHR-mCherry. (b) Viral constructs for the f-FLiCRE labelling paradigm were injected into the ventral CA1. (c) Example histology

of vCA1 f-FLiCRE labelling. Cells infected with the f-FLiCRE system will express GFP, while cells which are tagged during labelling will express mCherry. (d) Behavioural timeline to investigate the role of ventral CA1 ensembles that are active during context presentation alone (pre-loom labelling) and during looming and shock stimuli presentation (loom labelling). (e) Freezing responses pre- and post-looming stimulus on each test day for the pre-loom labelled cohort (repeated measures ANOVA with post-hoc comparisons; n = 6 mice). (f) Freezing responses pre- and post-looming stimulus onset on each test day for the loom-labelled cohort (repeated measures ANOVA with post-hoc comparisons; n = 6 mice). (g) Behavioural timeline to investigate the role of ventral CA1 ensembles that are active during naïve looming stimulus presentation. (i) Freezing responses pre- and post-looming stimulus on each test day for the innate loom labelled cohort (repeated measures ANOVA with post-hoc comparisons; n = 6 mice). n.s. $p \geq 0.05$, * $p<0.05$. ** $p<0.01$

References

ALLEN, W. E., DENARDO, L. A., CHEN, M. Z., LIU, C. D., LOH, K. M., FENNO, L. E., RAMAKRISHNAN, C., DEISSEROTH, K. & LUO, L. 2017. Thirst-associated preoptic neurons encode an aversive motivational drive. *Science,* 357**,** 1149-1155.

BALL, W. & TRONICK, E. 1971. Infant responses to impending collision: Optical and real. *Science,* 171**,** 818-820.

BOUTON, M. E. 2004. Context and behavioral processes in extinction. *Learn Mem,* 11**,** 485-94.

BOUTON, M. E. & KING, D. A. 1983. Contextual control of the extinction of conditioned fear: Tests for the associative value of the context. American Psychological Association.

BURNETT, L. E., KOPPENSTEINER, P., SYMONOVA, O., MASSON, T., VEGA-ZUNIGA, T., CONTRERAS, X., RÜLICKE, T., SHIGEMOTO, R., NOVARINO, G. & JOESCH, M. 2024. Shared behavioural impairments in visual perception and place avoidance across different autism models are driven by periaqueductal grey hypoexcitability in Setd5 haploinsufficient mice. *PLoS Biol,* 22**,** e3002668.

CARLILE, P. A., PETERS, R. A. & EVANS, C. S. 2006. Detection of a looming stimulus by the Jacky dragon: selective sensitivity to characteristics of an aerial predator. *Animal Behaviour,* 72**,** 553-562.

DE VRIES, SASKIA E. J. & CLANDININ, THOMAS R. 2012. Loom-Sensitive Neurons Link Computation to Action in the Drosophila Visual System. *Current Biology,* 22**,** 353-362.

DENARDO, L. A., LIU, C. D., ALLEN, W. E., ADAMS, E. L., FRIEDMANN, D., FU, L., GUENTHNER, C. J., TESSIER-LAVIGNE, M. & LUO, L. 2019. Temporal evolution of cortical ensembles promoting remote memory retrieval. *Nat Neurosci,* 22**,** 460-469.

DENG, H., XIAO, X. & WANG, Z. 2016. Periaqueductal Gray Neuronal Activities Underlie Different Aspects of Defensive Behaviors. *J Neurosci,* 36**,** 7580-8.

EVANS, D. A., STEMPEL, A. V., VALE, R., RUEHLE, S., LEFLER, Y. & BRANCO, T. 2018. A synaptic threshold mechanism for computing escape decisions. *Nature,* 558**,** 590-594.

FADOK, J. P., KRABBE, S., MARKOVIC, M., COURTIN, J., XU, C., MASSI, L., BOTTA, P., BYLUND, K., MÜLLER, C., KOVACEVIC, A., TOVOTE, P. & LÜTHI, A. 2017. A competitive inhibitory circuit for selection of active and passive fear responses. *Nature,* 542**,** 96-100.

INGLE, D. J. & KARIN V, S. H. 1990. Visually Elicited Evasive Behavior in Frogs. *BioScience,* 40**,** 284-291.

JIMENEZ, J. C., BERRY, J. E., LIM, S. C., ONG, S. K., KHEIRBEK, M. A. & HEN, R. 2020. Contextual fear memory retrieval by correlated ensembles of ventral CA1 neurons. *Nature communications,* 11**,** 3492.
JOSSELYN, S. A. & TONEGAWA, S. 2020. Memory engrams: Recalling the past and imagining the future. *Science,* 367.
KIM, C. K., SANCHEZ, M. I., HOERBELT, P., FENNO, L. E., MALENKA, R. C., DEISSEROTH, K. & TING, A. Y. 2020. A Molecular Calcium Integrator Reveals a Striatal Cell Type Driving Aversion. *Cell,* 183**,** 2003-2019.e16.
KIM, E. J., HOROVITZ, O., PELLMAN, B. A., TAN, L. M., LI, Q., RICHTER-LEVIN, G. & KIM, J. J. 2013. Dorsal periaqueductal gray-amygdala pathway conveys both innate and learned fear responses in rats. *Proc Natl Acad Sci U S A,* 110**,** 14795-800.
KJELSTRUP, K. G., TUVNES, F. A., STEFFENACH, H.-A., MURISON, R., MOSER, E. I. & MOSER, M.-B. 2002. Reduced fear expression after lesions of the ventral hippocampus. *Proceedings of the National Academy of Sciences,* 99**,** 10825-10830.
LEE, K. H., TRAN, A., TURAN, Z. & MEISTER, M. 2020. The sifting of visual information in the superior colliculus. *eLife,* 9**,** e50678.
LENZI, S. C., COSSELL, L., GRAINGER, B., OLESEN, S. F., BRANCO, T. & MARGRIE, T. W. 2022. Threat history controls flexible escape behavior in mice. *Current Biology,* 32**,** 2972-2979.e3.
LIU, X., RAMIREZ, S., PANG, P. T., PURYEAR, C. B., GOVINDARAJAN, A., DEISSEROTH, K. & TONEGAWA, S. 2012. Optogenetic stimulation of a hippocampal engram activates fear memory recall. *Nature,* 484**,** 381-5.
MADISEN, L., ZWINGMAN, T. A., SUNKIN, S. M., OH, S. W., ZARIWALA, H. A., GU, H., NG, L. L., PALMITER, R. D., HAWRYLYCZ, M. J., JONES, A. R., LEIN, E. S. & ZENG, H. 2010. A robust and high-throughput Cre reporting and characterization system for the whole mouse brain. *Nature Neuroscience,* 13**,** 133-140.
MATHIS, A., MAMIDANNA, P., CURY, K. M., ABE, T., MURTHY, V. N., MATHIS, M. W. & BETHGE, M. 2018. DeepLabCut: markerless pose estimation of user-defined body parts with deep learning. *Nature neuroscience,* 21**,** 1281-1289.
MEDEROS, S., VISSERS, N., BLAKELY, P., CLOPATH, C. & HOFER, S. 2024. Overwriting an instinct: visual cortex instructs learning to suppress fear responses. *bioRxiv***,** 2024.07.31.605567.
ORTEGA-DE SAN LUIS, C., PEZZOLI, M., URRIETA, E. & RYAN, T. J. 2023. Engram cell connectivity as a mechanism for information encoding and memory function. *Current Biology,* 33**,** 5368-5380.e5.
PAVLOV, P. I. 1927. Conditioned reflexes: An investigation of the physiological activity of the cerebral cortex. *Ann Neurosci,* 17**,** 136-41.
PEIRCE, J. W. 2009. Generating stimuli for neuroscience using PsychoPy. *Frontiers in Neuroinformatics,* 2.
POUGET, C., MORIER, F., TREIBER, N., GARCÍA, P. F., MAZZA, N., ZHANG, R., REEVES, I., WINSTON, S., BRIMBLE, M. A., KIM, C. K. & VETERE, G. 2024. Deconstruction of a memory engram reveals distinct ensembles recruited at learning. *bioRxiv***,** 2024.12.11.627894.
RESCORLA, R. A. 2004. Spontaneous Recovery. *Learning & Memory,* 11**,** 501-509.
RYAN, T. J., ORTEGA DE SAN LUIS, C., PEZZOLI, M. & SEN, S. 2021. Engram Cell Connectivity: An Evolving Substrate for Information Storage. *Current Opinion in Neurobiology*.
SCHIFF, W., CAVINESS, J. A. & GIBSON, J. J. 1962. Persistent fear responses in rhesus monkeys to the optical stimulus of" looming". *Science,* 136**,** 982-983.
SEMON, R. W. 1921. *The mneme,* London, Allen & Unwin.
SHANG, C., CHEN, Z., LIU, A., LI, Y., ZHANG, J., QU, B., YAN, F., ZHANG, Y., LIU, W., LIU, Z., GUO, X., LI, D., WANG, Y. & CAO, P. 2018. Divergent midbrain circuits orchestrate escape and freezing responses to looming stimuli in mice. *Nature Communications,* 9**,** 1232.

SHPOKAYTE, M., MCKISSICK, O., GUAN, X., YUAN, B., RAHSEPAR, B., FERNANDEZ, F. R., RUESCH, E., GRELLA, S. L., WHITE, J. A., LIU, X. S. & RAMIREZ, S. 2022. Hippocampal cells segregate positive and negative engrams. *Communications Biology,* 5**,** 1009.

TONEGAWA, S., PIGNATELLI, M., ROY, D. S. & RYAN, T. J. 2015. Memory engram storage and retrieval. *Curr Opin Neurobiol,* 35**,** 101-9.

TOVOTE, P., ESPOSITO, M. S., BOTTA, P., CHAUDUN, F., FADOK, J. P., MARKOVIC, M., WOLFF, S. B. E., RAMAKRISHNAN, C., FENNO, L., DEISSEROTH, K., HERRY, C., ARBER, S. & LÜTHI, A. 2016. Midbrain circuits for defensive behaviour. *Nature,* 534**,** 206-212.

VALE, R., CAMPAGNER, D., IORDANIDOU, P., AROCAS, O. P., TAN, Y. L., STEMPEL, A. V., KESHAVARZI, S., PETERSEN, R. S., MARGRIE, T. W. & BRANCO, T. 2020. A cortico-collicular circuit for accurate orientation to shelter during escape. *bioRxiv***,** 2020.05.26.117598.

WANG, Y.-C., JIANG, S. & FROST, B. J. 1993. Visual processing in pigeon nucleus rotundus: Luminance, color, motion, and looming subdivisions. *Visual Neuroscience,* 10**,** 21-30.

YILMAZ, M. & MEISTER, M. 2013. Rapid innate defensive responses of mice to looming visual stimuli. *Current biology : CB,* 23**,** 2011-2015.

ZAKI, Y., MAU, W., CINCOTTA, C., MONASTERIO, A., ODOM, E., DOUCETTE, E., GRELLA, S. L., MERFELD, E., SHPOKAYTE, M. & RAMIREZ, S. 2022. Hippocampus and amygdala fear memory engrams re-emerge after contextual fear relapse. *Neuropsychopharmacology,* 47**,** 1992-2001.

Acknowledgements

We thank Tamara Boto, Mani Ramaswami, and Ryan Lab members for useful scientific discussions and support.

Funding

This work was funded by the Air Force Office of Scientific Research (FA9550-24-1-0258), European Research Council (715968), Irish Research Council (GOIPG/2021/1331), Science Foundation Ireland (15/YI/3187), and Trinity College Dublin.

Author contributions

P.C., A.H., L.A., and T.J.R. conceived the scientific design.
P.C., L.A. and A.H. conducted the experiments, with assistance from A.M.Z, A.T. and J.O.L.
P.C. analysed the data, with input from L.A.
M.B. and S.W. produced the f-FLiCRE viral constructs.
Funding acquisition: T.J.R.
Project administration: P.C. and T.J.R.
P.C., L.A., A.M.Z., A.H., C.O.S., J.O.L, G.V., T.J.R. all contributed to interpretation of the results.
P.C. and T.J.R wrote the original manuscript draft.
P.C., L.A., A.M.Z., C.O.S., J.O.L, G.V., T.J.R. all contributed to reviewing and editing the manuscript.

Inclusion and Diversity

We support inclusive, diverse, and equitable conduct of research.

Supplementary material

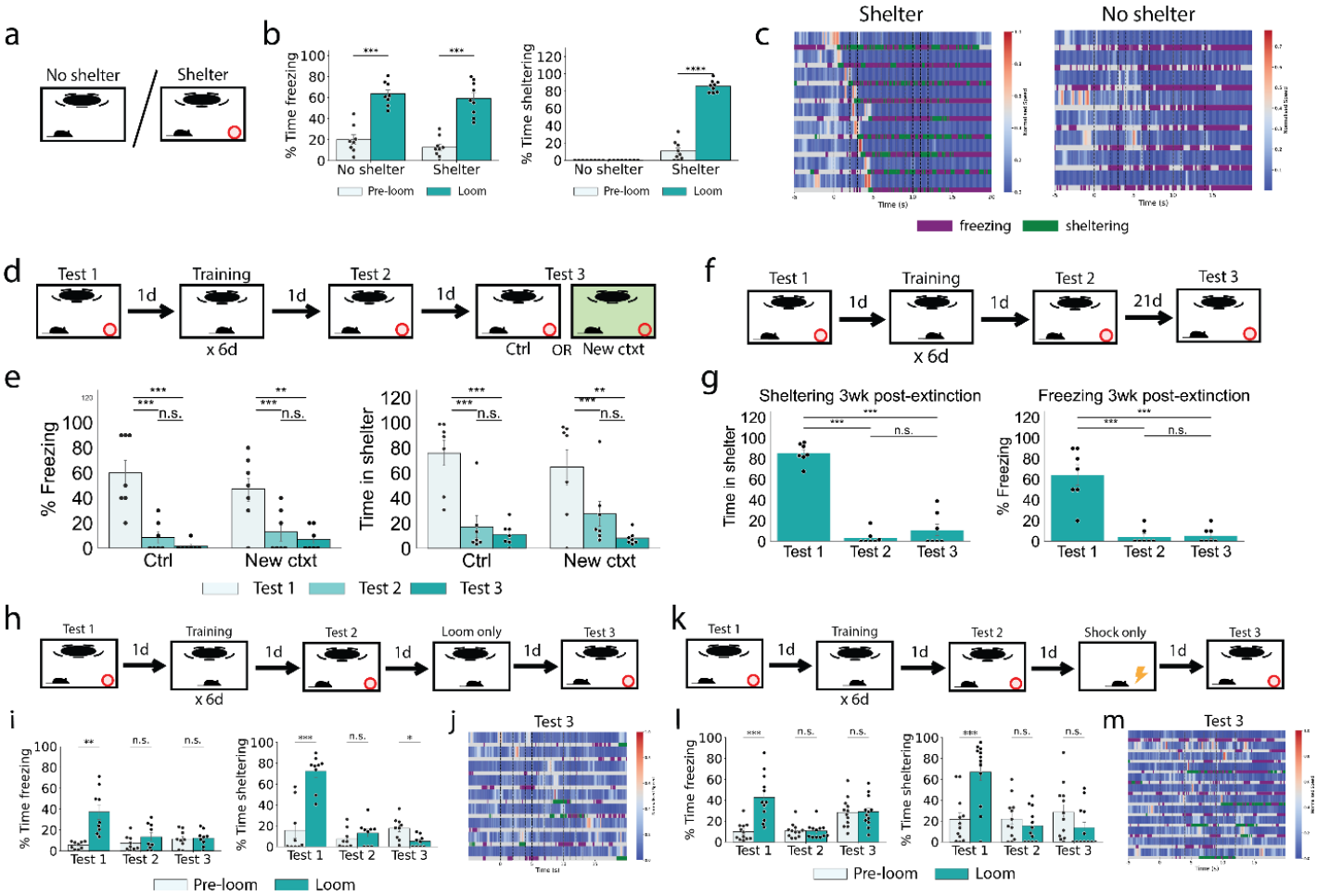

Supplementary figure 1 Looming extinction lasts at least 3 weeks, generalises to other contexts, and does not reinstate with a shock or loom stimulus provided separately. (a) Behavioural paradigm to compare looming responses with and without a shelter. (b) Freezing and sheltering behaviour of mice 15s pre- versus 15s post-stimulus onset both with and without the presence of a shelter (Student's T test; No shelter, n = 8 mice; Shelter, n = 9 mice). (c) Heatmap indicating the speed of mice, with each blue-red row indicating the speed of a single mouse. Beneath the speed, a bar indicates whether the individual mouse was detected as freezing (purple) or sheltering (green). (d) Extinction-renewal assessment paradigm. (e) Freezing and sheltering behaviour across test days in the extinction-renewal paradigm (Tukey's pairwise comparisons; ctrl, n = 7 mice; new context, n = 7 mice). (f) Extinction-spontaneous recovery assessment paradigm. (g) Freezing and sheltering behaviour in the extinction-spontaneous recovery paradigm (Tukey's pairwise comparison; n = 7 mice). (h) Extinction-reinstatement training paradigm with only the looming stimulus. (i) Freezing and sheltering responses of mice from the "loom only" cohort (Repeated measures ANOVA and posthoc Student's paired T test; n = 9 mice). (j) Heatmap indicating the speed of mice, with each blue-red row indicating the speed of a single mouse. (k) Extinction-reinstatement training paradigm with only the shock stimulus. (l) Freezing and sheltering responses of mice from the "shock only" cohort (Repeated measures ANOVA and posthoc Student's paired t test; n = 12 mice). (m) Heatmap indicating the speed of mice, with each blue-red row indicating the speed of a single mouse. n.s. p≥0.05, * p<0.05, **p<0.01, ***p<0.001

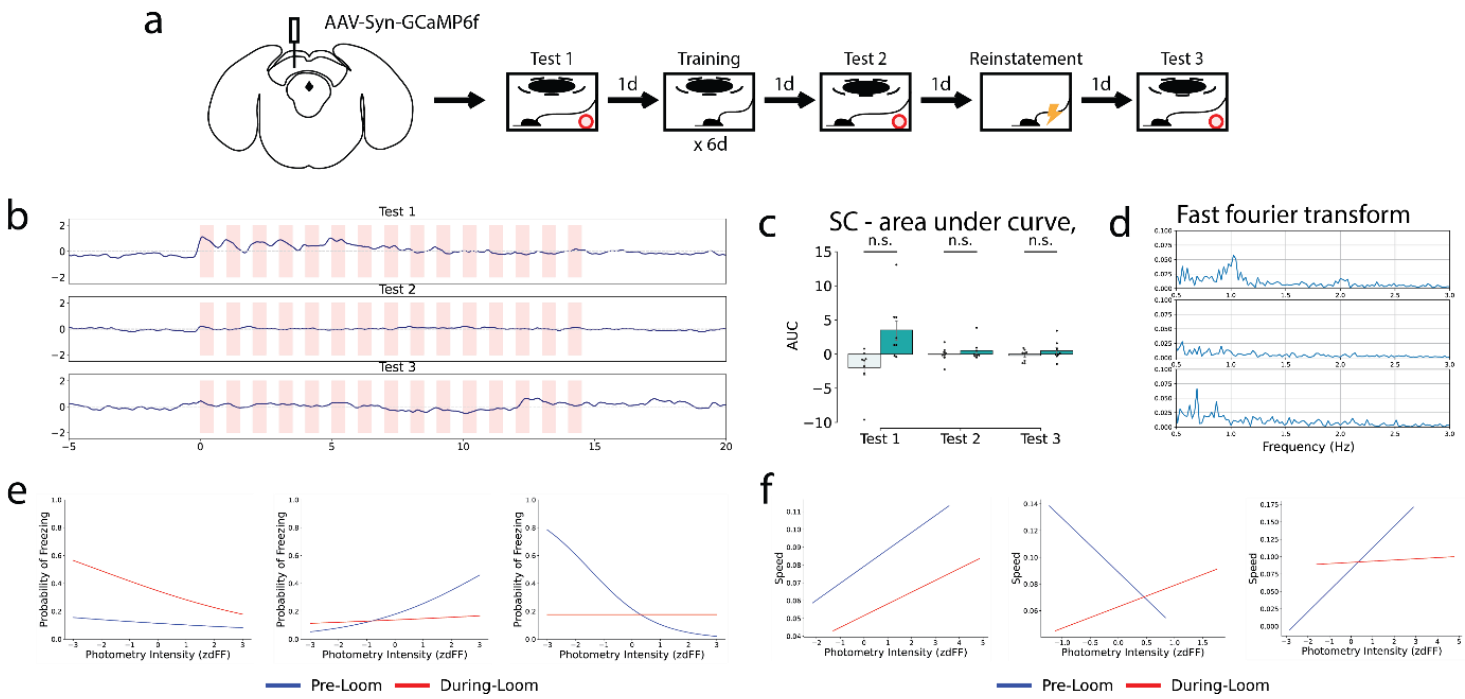

Supplementary figure 2 Fiber photometry recordings of the SC for mice undergoing the "shock only" reinstatement paradigm. (a) GCaMP was virally expressed in the SC. Fiber photometric recordings of GCaMP fluorescence were taken over the course of the extinction-reinstatement training paradigm. (b) Mean traces of calcium activity in the deep SC on each test day (n = 8 mice). (c) Area under curve of GCaMP signal 15s pre- and post-stimulus onset, for each day (Student's T test). (d) Fast Fourier transform of the GCaMP signal during stimulus presentation on each day. The most ethologically relevant peak occurs is at 1Hz, which is the frequency of looming stimulus presentation. (e) Logistic regression of freezing with GCaMP signal, 15s pre- and post-stimulus onset, for each test day. (f) Linear regression of speed with GCaMP signal, 15s pre- and post-stimulus onset, for each day. n.s. $p \geq 0.05$, *$p<0.05$

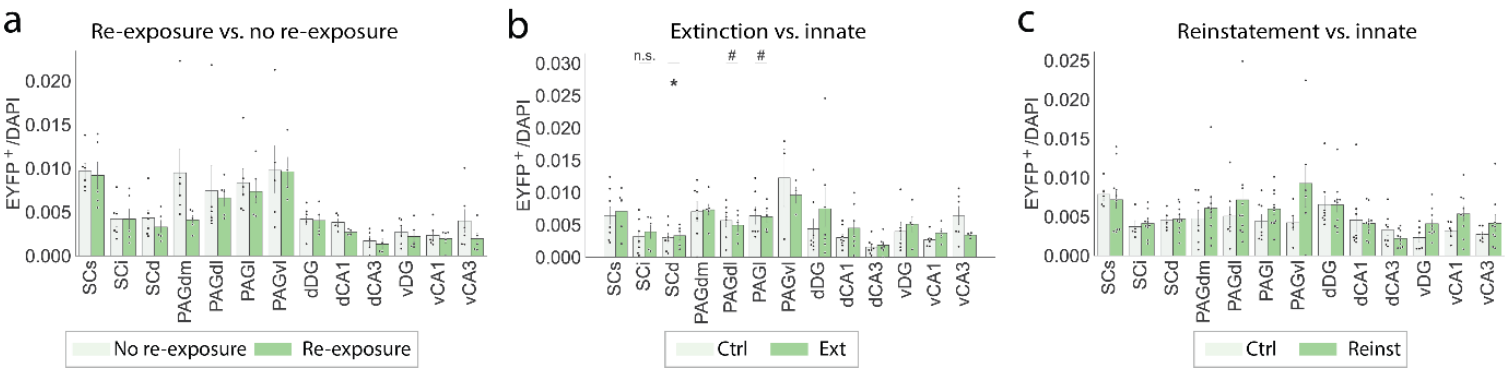

Supplementary figure 3 EYFP tagged cells in response to looming stimuli. (a) Number of engram cells tagged during looming for the re-exposure (n = 6 mice) vs. no re-exposure (n = 6 mice) paradigm (Student's paired t test with False discovery rate correction). (b-c) As in a, but for (b) extinction (n = 7 mice) vs. innate (n = 8 mice), and (c) reinstatement (n = 11 mice) vs. innate (n = 8 mice). n.s. $p \geq 0.05$, # $p < 0.05$, * $q < 0.05$; where p is the Student's t test p value, and q is the false discovery rate-adjusted p value.

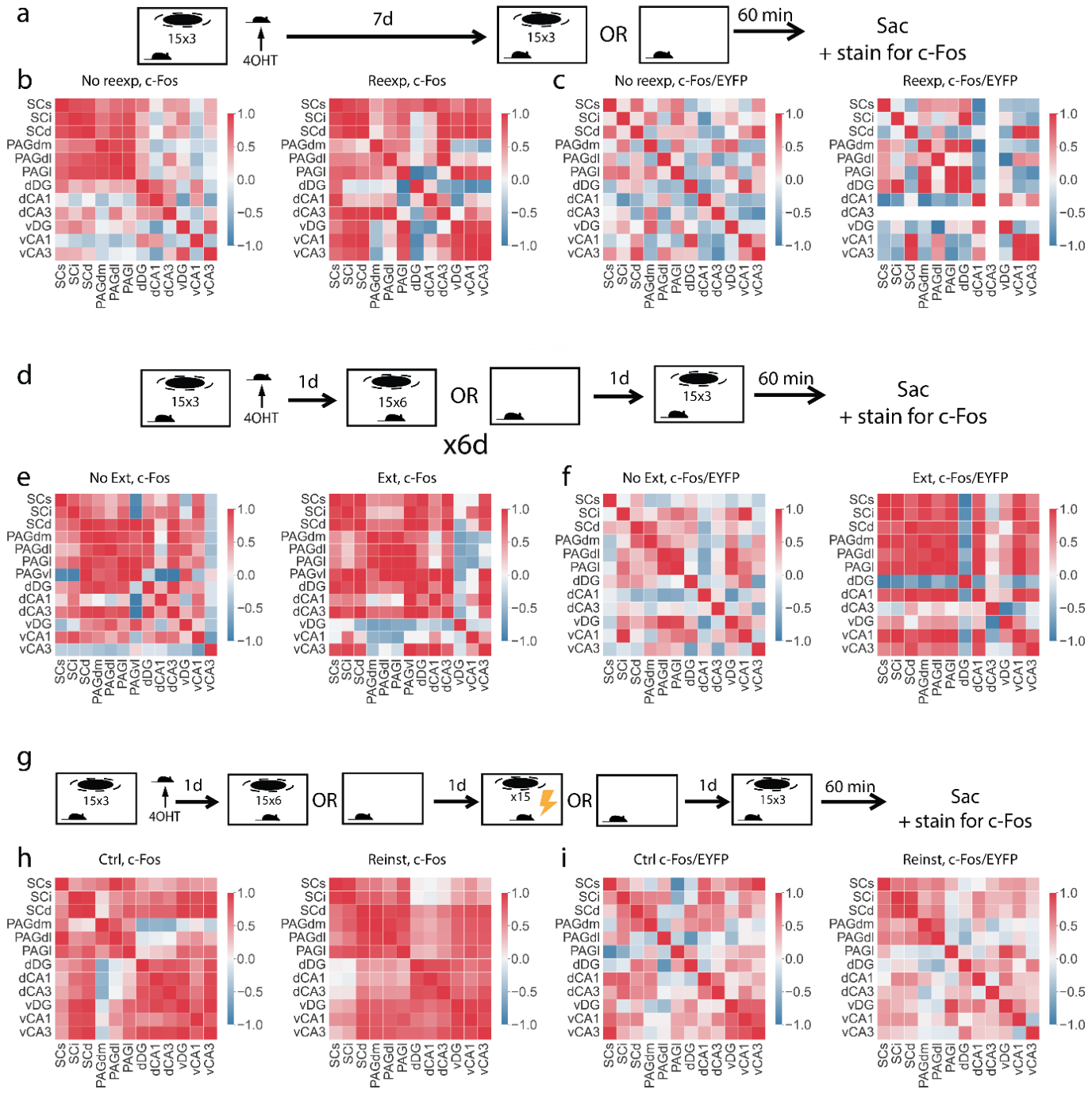

Supplementary figure 4 Correlation of c-Fos expression and engram reactivation in the midbrain and hippocampus during looming. (a) TRAP2xAi32 mice underwent re-exposure (n = 6 mice) or no re-exposure (n = 6 mice) Mice were injected with 4-OHT to transiently induce c-Fos dependent EYFP upon first exposure to the looming stimulus, and later perfused 60min following stimulus presentation at the end of the behavioural paradigm. (b) Correlations in c-Fos expression for mice undergoing no re-exposure vs. re-exposure. (c) Correlations in engram re-activation for mice undergoing no re-exposure vs. re-exposure. (d-f) As in a-c, but for mice with innate responses (n = 6 mice) vs. extinction (n = 7 mice). (g-i) As in a-c, but for mice with innate responses (n = 8 mice) vs. reinstatement (n = 11 mice).

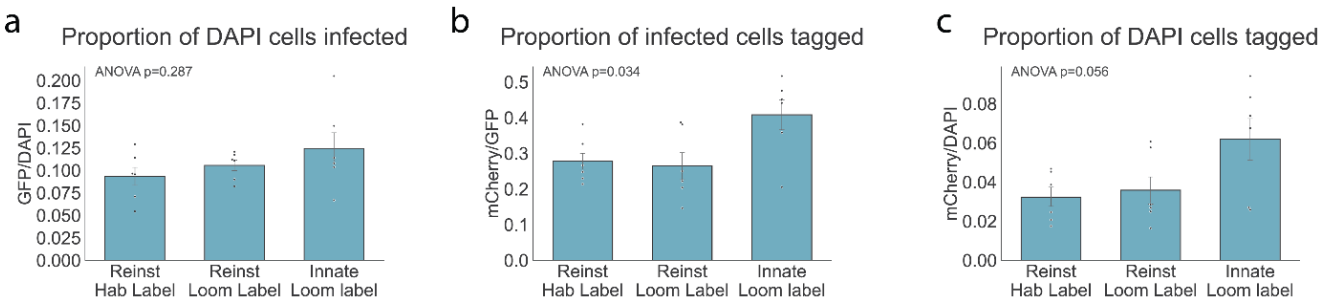

Supplementary figure 5 f-FLiCRE labelling quantification. (a) The proportion of DAPI cells which were infected with the f-FLiCRE construct (n = 6 mice). (b) The proportion of infected cells tagged during stimulus presentation (n = 6 mice). (c) The proportion of DAPI cells tagged during stimulus presentation (n = 6 mice).